

Optics Letters

Simultaneous two-plane flame front detection using PIV based on defocusing

QICHI HE,*  CHRISTOPHER WILLMAN, AND BENJAMIN A. O. WILLIAMS

Department of Engineering Science, University of Oxford, Oxford OX1 3PJ, United Kingdom

*qichi.he@eng.ox.ac.uk

Received 14 September 2023; revised 22 November 2023; accepted 8 December 2023; posted 11 December 2023; published 14 January 2024

This Letter presents a simultaneous two-plane flame front detection method. It is based on a standard single-camera single-plane particle image velocimetry (PIV) system in combination with an inexpensive and compact image splitting device. The image splitting optics places images from two depth-offset planes onto the two halves of a camera sensor. A shallow depth of field ensures only one plane is in focus on each half of the sensor. By using a high-pass filter and a novel two-step filter we have devised, the out-of-focus particle images are effectively removed, while the in-focus particle images remain, allowing the turbulent flame fronts on two planes to be detected simultaneously. Our approach could be combined with conventional polarization/wavelength discrimination methods to achieve simultaneous multi-plane flame front reconstruction with similarly high in-plane spatial resolution to single-plane measurement and is suitable for practical combustion devices with limited optical access.

Published by Optica Publishing Group under the terms of the [Creative Commons Attribution 4.0 License](https://creativecommons.org/licenses/by/4.0/). Further distribution of this work must maintain attribution to the author(s) and the published article's title, journal citation, and DOI.

<https://doi.org/10.1364/OL.503534>

Turbulent premixed combustion is of great interest for industrial applications where low pollutant emissions are sought. It is well-established that most premixed turbulent flames that have been studied to date are composed of wrinkled “flamelets” [1]. In the so called flamelet regime, the thickness of the chemical reaction layer (flame front) is smaller than the Kolmogorov scale [2]. The flame can be regarded as behaving similarly to the laminar case and described independently of the turbulent flow field. Fundamental parameters such as the flame surface density, flame brush thickness, and turbulent burning velocity are calculated based on the turbulent flame front [3]. These parameters are not only significant to a better understanding of the underlying mechanisms of turbulent premixed combustion, but also useful for validating computational models.

The measurement of flame front position relies on laser based optical diagnostics techniques. The laser induced fluorescence (LIF) signal from radicals such as OH and CH, which are generated during combustion, is frequently used for flame front tracking [4–7]. Another common approach adapts particle image velocimetry (PIV, also called Conditioned PIV when it was first

proposed for flame front extractions and in some later publications) [8,9]. It works by detecting the sharp particle number density gradient in the Mie-scattering images of the seeding particles, caused by the temperature change between the unburned and burned regions. It was proposed as a low-cost and reliable alternative for flame front detection, and has been applied widely [8–13]. Besides, the PIV method can achieve simultaneous measurement of flame front position and flow velocity field, enabling relatively simple determination of flow–flame interaction and flame displacement speed without needing an additional LIF system [10,11]. In principle, flame front measured by PIV is in the preheat layer where the sharp temperature gradients exist (slightly toward reactants). Radicals like OH and CH are post-flame species (slightly toward products).

Conventionally, the above-mentioned techniques deliver single-plane measurements. Efforts have been made to capture the three-dimensional (3D) information of flame front structure. One representative example is volumetric LIF imaging based on tomographic reconstruction [14,15]. In a combustion device where optical access is limited, such as the optically accessible internal combustion engine described in this Letter, deploying a camera array for an accurate tomographic reconstruction is impractical. Alternatively, researchers record signals from multiple planes by laser sheet scanning across the volume of interest, thereby recovering the 3D structure of the flame or investigating correlations between planes [16–19]. The sequential nature of scanning measurement may restrict the application to moderate flow rates and turbulence levels. Simultaneous multi-plane measurements have been attempted, by using the polarization and wavelength differences of the light [20,21]. They can achieve simultaneous measurements with high spatiotemporal resolution, but the number of measurement planes is limited.

In this Letter, we present a simultaneous two-plane flame front measurement using PIV. It is based on a standard single-plane PIV system in combination with an image splitting device. Our previous work validated the feasibility and accuracy of using this configuration for a simultaneous two-plane velocimetry of non-reacting flows [22,23]. By using a non-polarizing beam splitter and mirrors with adjustable optical path lengths, each half of a camera sensor is focused to a different depth plane. With a shallow depth of field, the overlapping image that is not in-focus is significantly defocused. Based on a high-pass filter and a novel two-step filter we have devised, the out-of-focus particle images

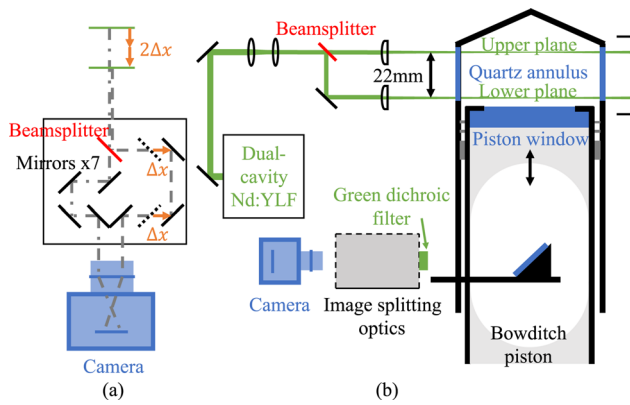


Fig. 1. (a) The image splitting device (adapted from [22]). (b) Two-plane flame front detection in the optical engine.

can be effectively removed while the in-focus particle images remain. Potentially, by further splitting the images, or combining our method with conventional polarization/wavelength discrimination, simultaneous flame front detection on more planes could be achieved. The focus of this Letter is to demonstrate our method, and to assess the flame front detection uncertainty caused by two-plane cross talk.

The image splitting optics design is shown in Fig. 1 (a). A 2-in. 50/50 non-polarizing beam splitter (Thorlabs BSW42-532) splits scattered light from two parallel depth-offset planes into two paths. Mirrors are used to direct light traveling along each path to a different half of the camera sensor. Since both optical

paths share the same camera lens and image distance, by adjusting the positions of the mirrors (therefore the optical path length of each path), the two measurement planes can be placed at different depths along the optical axis. For either side of the camera sensor, the image from one plane is in-focus, while the other plane's image is out-of-focus. By using a large aperture camera lens ($f = 85\text{mm}, f/2$), a shallow depth of field is achieved.

The two-plane flame front measurement was performed in a single-cylinder, optically accessible gasoline direct injection engine (Fig. 1 (b)). The engine ran at 1000 revolutions per minute (RPM) with stoichiometric isooctane-air mixtures. A LaVision aerosol generator was used to seed olive oil droplets into the intake plenum. A pair of coaxial laser beams, generated by a dual-cavity Nd:YLF laser (Photonics Industries DM20-527-DH), were split into two pairs by a 50/50 non-polarizing beam splitter (Edmund Optics 35959). A fused silica annulus provided optical access for the laser sheets, illuminating two horizontal planes in the engine. The upper plane was 2.5 mm below the firing deck. The lower plane was 22 mm below the upper plane. A Bowditch piston and 45° mirror arrangement enabled the planes to be imaged through the piston crown window onto a high-speed CMOS camera (Phantom VEO 710L). A dichroic filter (Elliot Scientific CDG-5051) was used to reject chemiluminescence emission from the flame, and transmit the green Mie scattering from the PIV particles. The field of view on each plane was 35 mm \times 107 mm. Restriction of the field of view size, caused by the image splitting optics, is discussed in [22].

Figure 2 presents two examples of detecting flame fronts on the two planes. To improve visualization, all PIV images presented in this Letter are rotated so that the upper-plane image and

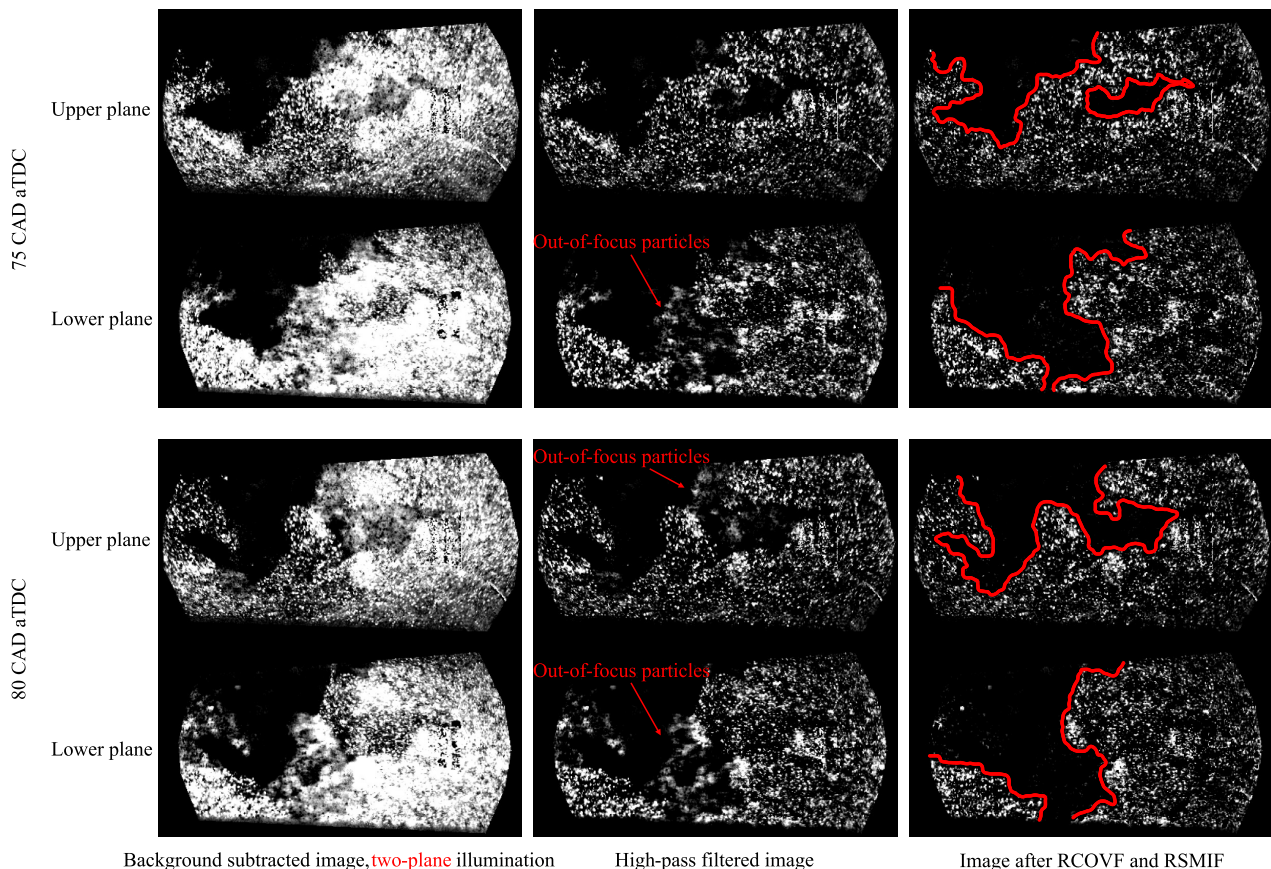


Fig. 2. Two-plane flame front detection examples.

lower-plane image are vertically arranged. Row 1 shows images at 75 crank angle degrees (CAD) after Top Dead Centre (aTDC), and Row 2 shows images at 80 CAD aTDC, in the same cycle. The first column shows background subtracted images. The second column presents images processed with a high-pass filter, which subtracted the images' low-frequency content generated using a 2D Gaussian smoothing kernel (32×32 pixels in this work). It is noticed that the high-pass filter is able to remove a substantial fraction of the out-of-focus particle images, but some still remain. Here we propose a two-step filter to clean up the blurry particle images. The first step is called a ratiometric coefficient of variation filter (RCOVF). First, a 5×5 window is used to calculate the local coefficient of variation for each pixel:

$$C_v(i, j) = \frac{\sigma(i-2:i+2, j-2:j+2)}{\mu(i-2:i+2, j-2:j+2)}, \quad (1)$$

in which i and j denote the pixel's coordinates, σ and μ refer to standard deviation and mean. In an area where only out-of-focus particle images exist, the local coefficient of variation is much smaller than that in areas where in-focus particles appear. Note that if out-of-focus particles are seen on one of the two planes, corresponding in-focus particles are then found

Algorithm 1. Ratiometric coefficient of variation filter (RCOVF)

```

1: procedure RCOVF( $i_u, j_u$ )           ▷ Filter the upper-plane image
   (subscript  $u$ )
2:   if  $\frac{C_v(i_u, j_u)}{C_v(i_l, j_l)} < 0.5$  then
3:      $I(i_u, j_u) = 0$ 
4: procedure RCOVF( $i_l, j_l$ )           ▷ Filter the lower-plane image
   (subscript  $l$ )
5:   if  $\frac{C_v(i_l, j_l)}{C_v(i_u, j_u)} < 0.5$  then
6:      $I(i_l, j_l) = 0$ 

```

on the other plane in a region which has the same in-plane world coordinates. That means for areas where particles exist on both planes, the local coefficient of variation values in both images are similar. For areas where particles only exist on one of the two planes, the local coefficient of variation values from both images should have a relatively large difference. Therefore the ratio of the local coefficient of variation from both images can be used to remove certain pixels considered to contain only out-of-focus particle images, by applying the RCOVF defined in Algorithm 1.

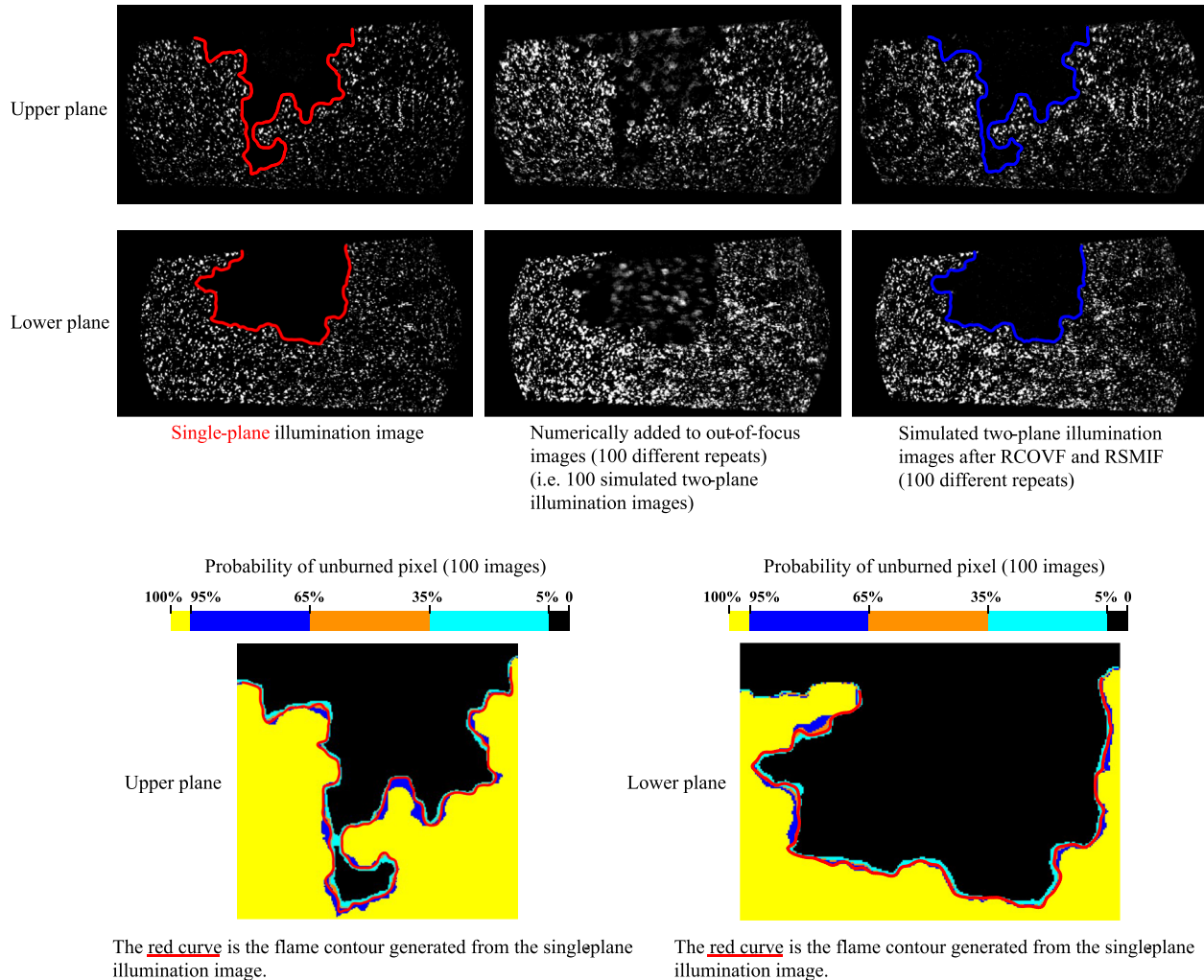


Fig. 3. Evaluation of flame front detection uncertainty caused by out-of-focus images. The last row shows the probability density map of the unburned region of each plane calculated from the numerically added images, overlaid with flame contour generated from the single-plane illumination image.

Algorithm 2. Ratiometric sliding maximum intensity filter (RSMIF)

```

1: procedure RSMIF( $i_u, j_u$ )           ▶ Filter the upper-plane image
   (subscript  $u$ )
2:   if  $\frac{S(i_u, j_u)}{S(i_l, j_l)} < 0.5$  and  $\frac{C_v(i_u, j_u)}{C_v(i_l, j_l)} < 1$  then
3:      $I(i_u, j_u) = 0$ 
4: procedure RSMIF( $i_l, j_l$ )           ▶ Filter the lower-plane image
   (subscript  $l$ )
5:   if  $\frac{S(i_l, j_l)}{S(i_u, j_u)} < 0.5$  and  $\frac{C_v(i_l, j_l)}{C_v(i_u, j_u)} < 1$  then
6:      $I(i_l, j_l) = 0$ 

```

In practice, the RCOVF performs well in removing the central part of an out-of-focus image “blob”, but it is not able to effectively remove the edges of the out-of-focus particle images. Therefore, a second step called ratiometric sliding maximum intensity filter (RSMIF) is applied. It is based on the observation that for those bright out-of-focus particles which survive high-pass filtering, there should be corresponding bright in-focus particles on the other plane. The filter is defined in Algorithm 2, where S is the sliding maximum intensity value of each pixel calculated using a 13×13 window:

$$S(i, j) = \max \{I(i - 6 : i + 6, j - 6 : j + 6)\}. \quad (2)$$

In this filter, the ratio of the sliding maximum intensity value is used to evaluate if a pixel is a part of the edge of an out-of-focus particle image. Due to the inherent brightness difference of in-focus particle images, caused by, e.g., the different physical sizes of in-focus particles and the spatial distribution of laser sheet energy, the second condition on the coefficient of variation ratio is used to prevent removing pixels in regions where in-focus particles exist on both planes.

The effect of the proposed two-step filter is visualized in the third column of Fig. 2. Direct observation of the images shows that the out-of-focus particles were removed satisfactorily. Based on the filtered images, turbulent flame front contours were determined using the automatic histogram-based threshold approach proposed by [8].

To evaluate the flame front detection uncertainty caused by two-plane cross talk, single-plane illumination images were numerically added, so that we are able to compare the flame front contours generated from the numerically added “two-plane illumination” images and from the ground-truth single-plane illumination images. In Fig. 3, a single-plane (upper and lower) illumination image was selected and numerically added to 100 others to create 100 “two-plane illumination” images. In the last row of Fig. 3, the probability density map of the unburned region of each plane calculated from the numerically added images is presented, and the flame contour generated from the single-plane illumination image is overlaid. We observe that despite the cross talk imposed during numerical addition, the algorithm remains able to extract the structure of the flame front highly reproducibly.

In summary, we have proposed a simultaneous two-plane flame front detection method using defocusing based PIV. It could be applied alone as an inexpensive approach to extend a standard single-plane PIV system for two-plane measurement, or combined with conventional polarization/wavelength

discrimination to achieve simultaneous multi-plane flame front reconstruction. Our previous work [22] indicated that reliable flow velocity field reconstructions of non-reacting flows could be achieved with plane separation as small as 15 mm, with the same optical hardware and similar field of view size to this work. In future work we will systematically investigate the impact of plane separation on flame front measurement and study the achievable improvement by narrowing camera depth of field and optimizing image processing steps.

Funding. Engineering and Physical Sciences Research Council (EP/T005327/1).

Acknowledgments. This research was funded in whole or in part by an Engineering and Physical Sciences Research Council Prosperity Partnership, grant number EP/T005327/1. The Prosperity Partnership is a collaboration between Jaguar Land Rover, Siemens Digital Industries Software, the University of Bath and the University of Oxford.

Disclosures. The authors declare no conflicts of interest.

Data availability. Due to confidentiality agreements with research collaborators, data underlying the results presented in this paper can only be made available to bona fide researchers subject to a non-disclosure agreement. Details of the data and how to request access are available from the corresponding author.

REFERENCES

- J. F. Driscoll, J. H. Chen, A. W. Skiba, *et al.*, *Prog. Energy Combust. Sci.* **76**, 100802 (2020).
- N. Peters, *Turbulent Combustion*, Cambridge Monographs on Mechanics (Cambridge University Press, 2000).
- J. F. Driscoll, *Prog. Energy Combust. Sci.* **34**, 91 (2008).
- I. Boxx, C. Slabaugh, P. Kutne, *et al.*, *Proc. Combust. Inst.* **35**, 3793 (2015).
- A. Jain, P. Parajuli, Y. Wang, *et al.*, *Opt. Lett.* **45**, 4690 (2020).
- P. S. Hsu, M. N. Slipchenko, N. Jiang, *et al.*, *Opt. Lett.* **45**, 5776 (2020).
- M. Tanahashi, S. Murakami, G.-M. Choi, *et al.*, *Proc. Combust. Inst.* **30**, 1665 (2005).
- S. Pfadler, F. Beyrau, and A. Leipertz, *Opt. Express* **15**, 15444 (2007).
- X. Wang, K. Liu, C. Fu, *et al.*, *Exp. Fluids* **64**, 118 (2023).
- P. G. Aleiferis and M. K. Behringer, *Combust. Flame* **162**, 4533 (2015).
- C. Mounaïm-Rousselle, L. Landry, F. Halter, *et al.*, *Proc. Combust. Inst.* **34**, 2941 (2013).
- Y. Zheng, L. Weller, and S. Hochgreb, *Exp. Fluids* **63**, 79 (2022).
- S. Pfadler, F. Dinkelacker, F. Beyrau, *et al.*, *Combust. Flame* **156**, 1552 (2009).
- B. R. Halls, N. Jiang, T. R. Meyer, *et al.*, *Opt. Lett.* **42**, 2830 (2017).
- L. Ma, Q. Lei, T. Capil, *et al.*, *Opt. Lett.* **42**, 267 (2017).
- R. Wellander, M. Richter, and M. Aldén, *Exp. Fluids* **55**, 1 (2014).
- J. Weinkauff, M. Greifenstein, A. Dreizler, *et al.*, *Meas. Sci. Technol.* **26**, 105201 (2015).
- Z. Yang, S. Wang, J. Zheng, *et al.*, *Opt. Lett.* **45**, 5756 (2020).
- J. Bode, J. Schorr, C. Krüger, *et al.*, *Proc. Combust. Inst.* **37**, 4929 (2019).
- M. Shimura, T. Ueda, G.-M. Choi, *et al.*, *Proc. Combust. Inst.* **33**, 775 (2011).
- B. Peterson, E. Baum, A. Dreizler, *et al.*, *Combust. Flame* **202**, 16 (2019).
- Q. He, C. Willman, R. Stone, *et al.*, *Phys. Fluids* **35**, 067122 (2023).
- C. Willman, Q. He, B. A. O. Williams, *et al.*, “Multi-plane PIV using depth of field for in-cylinder flow measurements,” SAE Technical Papers **2023-01-0213** (2023).